

Optical Engineering

SPIDigitalLibrary.org/oe

Universal optical line terminal encoding and decoding architecture in two-code keying for noncoherent spectral amplitude coding optical code division multiple access systems

Bih-Chyun Yeh
Cheing-Hong Lin
De-Nian Yang

Universal optical line terminal encoding and decoding architecture in two-code keying for noncoherent spectral amplitude coding optical code division multiple access systems

Bih-Chyun Yeh,* Cheing-Hong Lin, and De-Nian Yang

Chung Gung University, Department of Electrical Engineering, Taiwan, China

Abstract. We propose a new code family, called extended shifted prime codes, and the universal encoding architecture for spectral amplitude coding optical code division multiple access systems using a two-code keying scheme. The proposed system can eliminate multiuser interference and suppress phase-induced intensity noise. In addition, we design the ESP codes to be an encoding/decoding architecture based on the array waveguide grating architecture and reduce the power loss and the complexity of the optical line terminal. The numerical results demonstrate that the proposed system with ESP codes outperforms the existing one-dimensional shifted prime codes system. © The Authors. Published by SPIE under a Creative Commons Attribution 3.0 Unported License. Distribution or reproduction of this work in whole or in part requires full attribution of the original publication, including its DOI. [DOI: 10.1117/1.OE.53.1.016104]

Keywords: array waveguide grating; optical code division multiple access; phase-induced intensity noise; passive optical network; shifted prime codes.

Paper 130750 received May 21, 2013; revised manuscript received Nov. 24, 2013; accepted for publication Dec. 6, 2013; published online Jan. 6, 2014.

1 Introduction

Optical code division multiple access (OCDMA) can provide high-speed connections with bandwidth sharing and secure communications in next-generation optical access networks.¹ Spectral amplitude coding (SAC) in OCDMA systems has been exploited in the optical networking units of passive optical networks (PONs).^{2,3} However, in the on-off keying, the codewords are unidimensional and require the codewords power of bit “1” and the zero codewords power of bit “0” to control the unequal power to accommodate more simultaneous users in PONs.⁴ The codewords in two-code keying (TCK) are a better event because the codewords power of bit “1” and the codewords power of bit “0” control the equal power. In addition, the performance of OCDMA systems is limited by the multiuser interference (MUI).⁵ To address this issue, shifted prime (SP) codes with TCK are proposed to remove MUI.⁶ In this letter, we propose extended shifted prime (ESP) codes with TCK to further reduce the phase-induced intensity noise (PIIN) and support more simultaneous users. The variance of PIIN current is effectively reduced by employing the proposed ESP codes. We also propose a novel array waveguide grating (AWG) architecture to decrease the power loss and complexity of the optical line terminal (OLT).

In the following sections, we first review the SP codes.⁶ The SP codes are designed to eliminate MUI without chip stuffing of the codes. A code sequence of the SP code is denoted as $C_{m,n} = [c_{m,n}(0), c_{m,n}(1), \dots, c_{m,n}(p-1)]$, where $m = 0, 1, \dots, p-1, n = 0, 1, \dots, p-1$, and $C_{m,n} \in p^p$. The p^p represents the set of all p -tuples over

GF(p). The corresponding codeword is denoted as $X_{m,n} = [x_{m,n}(0), x_{m,n}(1), \dots, x_{m,n}(p^2 - 1)]$. Therein, we set $x_{m,n}(i) = 1$ as $i = c_{m,n}(b) + bp$ and $b = 0, 1, \dots, p-1$, where $c_{m,n}(b) = m \bullet b \oplus n$. Otherwise, $x_{m,n}(i) = 0$. The \bullet and \oplus are the modulo- p multiplication and addition, respectively. The codewords $X_{m,n}$ with the same value m belong to the same code group. The cross-correlations between the two SP codewords $X_{m,n}$ and $X_{q,r}$ are $X_{m,n} \odot X_{q,r} = p$ as $m = q, n = r$, $X_{m,n} \odot X_{q,r} = 0$ as $m = q, n \neq r$, or $X_{m,n} \odot X_{q,r} = 1$ as $m \neq q$, where \odot is the dot-product of two vectors.

2 1-D ESP Codes with TCK

In the letter, we design ESP codes to reduce PIIN and increase the number of simultaneous users. Specifically, we describe the ESP codes as follows: $x_{e,m,n}(j) = 1$, for $j = (e-1)p + c_{m,n}(b) + bNp$, $b = 0, 1, \dots, p-1$; otherwise, $x_{e,m,n}(j) = 0$, where $e \in \{1, 2, \dots, N\}$. The code weight is p , the code length is Np^2 , the number of codewords is $M = Np^2$, and the code size is $M_s = N(p^2 - p)/2$. Table 1 uses an example with $N = 2$, $p = 3$, $M = 18$, and $M_s = 6$.

The cross-correlations of the ESP codes are specified as follows: $X_{e,m,n} \odot X_{f,q,r} = p$ as $e = f, m = q, n = r$, $X_{e,m,n} \odot X_{f,q,r} = 0$ as $e = f, m = q, n \neq r$, $X_{e,m,n} \odot X_{f,q,r} = 0$ as $e \neq f$, or $X_{e,m,n} \odot X_{f,q,r} = 1$ as $e = f, m \neq q$. Moreover, we let any two codewords ($X_{e,m,n}$ and $X_{e,m,n'}$), which belong to the same code group, assigned to the same user for TCK. It is set as $X_{e,m,n} = X_{e,m,n+1}$ in this letter. Table 1 uses a codeword $X_{e,m,n}$ or $X_{e,m,n}$ as the encoding of information bit “0” or “1”. The modified cross correlations in ESP codes for TCK are derived as follows:

*Address all correspondence to: Bih-Chyun Yeh, E-mail: bih.chyun.yeh@gmail.com

Table 1 Extended shifted prime (ESP) codes for $N = 2$, code weight $p = 3$, and code size $M_s = 6$.

e	m	n	$X_{e,m,n}$
1	0	0	100 000 100 000 100 000
1	0	1	010 000 010 000 010 000
1	0	2	001 000 001 000 001 000
1	1	0	100 000 010 000 001 000
1	1	1	010 000 001 000 100 000
1	1	2	001 000 100 000 010 000
1	2	0	100 000 001 000 010 000
1	2	1	010 000 100 000 001 000
1	2	2	001 000 010 000 100 000
2	0	0	000 100 000 100 000 100
2	0	1	000 010 000 010 000 010
2	0	2	000 001 000 001 000 001
2	1	0	000 100 000 010 000 001
2	1	1	000 010 000 001 000 100
2	1	2	000 001 000 100 000 010
2	2	0	000 100 000 001 000 010
2	2	1	000 010 000 100 000 001
2	2	2	000 001 000 010 000 100

$$\begin{aligned}
 & X_{e,m,n} \ominus X_{f,q,r} - X_{e,m,n'} \ominus X_{f,q,r} \\
 & = \begin{cases} p, & e = f, m = q, n = r, \\ -p & e = f, m = q, n' = r, \\ 0 & \text{otherwise.} \end{cases} \quad (1)
 \end{aligned}$$

The above subtraction method for TCK can eliminate MUI according to the difference between the two

correlations. For ESP scheme, we propose a new OLT as shown in Fig. 1, which includes a $1 \times M_s$ splitter at the remote node, and M_s optical network units (ONUs). The AWG architecture can effectively combine all codes into one and concentrate the power. The $ONU(\tau)$, where $\tau \in \{0, 1, \dots, M_s - 1\}$, is able to decode the ESP codes to produce the information bits “0” or “1” for user(τ). As shown in Fig. 1, the OLT transmitter includes a broadband light source (BLS), an AWG architecture, and a matrix operation circuit.

The AWG architecture includes one $1 \times Np^2$ AWG demultiplexer, Np^2 electro-optic modulators (EOMs), and one $Np^2 \times 1$ AWG multiplexer. The light outputted from BLS designs wavelength bandwidth to be first divided into Np^2 wavelength chips by the $1 \times Np^2$ AWG demultiplexer. The wavelengths of Np^2 wavelength chips are esignated as $\lambda_0, \lambda_1, \dots, \lambda_{Np^2-1}$. These wavelength chips are then modulated by the Np^2 EOMs, respectively. At last, these modulated wavelength chips are combined by the $Np^2 \times 1$ AWG multiplexer and outputted into an external fiber for data transmission. The EOM modulates the incoming wavelength chips according to the variables $h_0, h_1, \dots, h_{Np^2-1}$, which are calculated based on the information bits and adopted ESP codewords of each user via the matrix operation circuit. The calculation of this matrix operation circuit is performed according to $\mathbf{H} = 1/p \times \mathbf{S} \times \mathbf{BIT}$, where $\mathbf{H} = [h_0, h_1, \dots, h_{M-1}]^T$, $\mathbf{S} = [X_{1,0,0}^T, X_{1,0,1}^T, \dots, X_{N,p-1,p-1}^T, X_{N,p-1,p-2}^T]$, and $\mathbf{BIT} = [\text{bit}_0, \text{bit}_0, \dots, \text{bit}_{M_s-1}, \text{bit}_{M_s-1}]^T$. Therein, $X_{1,0,0}^T$ and $X_{1,0,1}^T$ are the transpose of codeword vectors for user #0, ..., and $X_{N,p-1,p-1}^T$ and $X_{N,p-1,p-2}^T$ are for user #($M_s - 1$). In fact, a universal OLT encoding architecture can be operated with other code families, e.g., SP codes and M^3 sequence codes.^{6,7} Only the codeword matrix \mathbf{S} needs to be updated.

The proposed transmitter encodes ESP codes in the electrical domain, the same as the literature,⁸⁻¹¹ and it has been shown that the EOM can transfer the electrical domain into the optical domain.¹²

In Fig. 2, the modulation voltage V_m is the input of EOM, and the optical transmitted intensity I_n is the output of the EOM, where the optical transmitted intensity $I_n = I_{n0} + \psi V_m$. If $V_m = 0$, the optical transmitted intensity

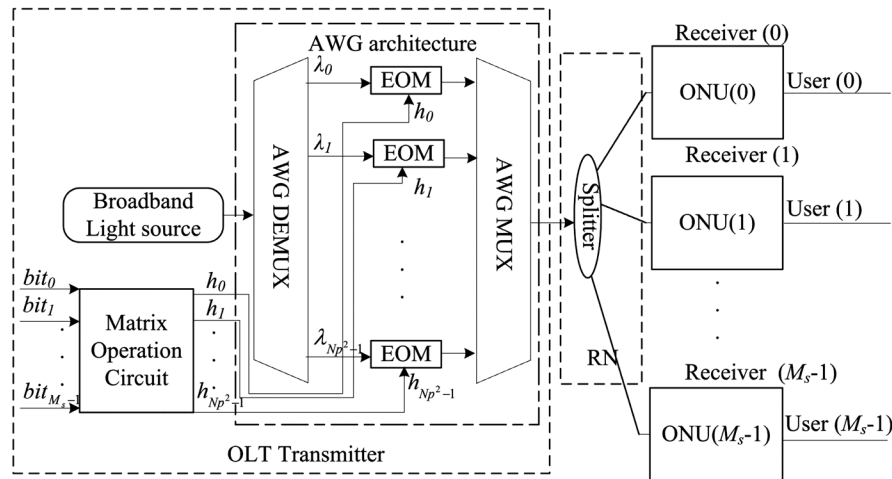


Fig. 1 Schematic block diagram of extended shifted prime (ESP) codes for two-code keying (TCK) including transmitter and receiver.

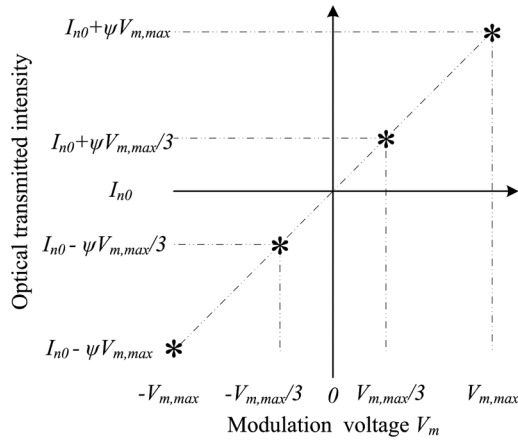


Fig. 2 The modulation voltage versus the optical transmitted intensity of the electro-optic modulator (EOM).

is I_{n0} . The EOM transfers the modulation voltage V_m into optical transmitted intensity I_n . Therefore, the ratio of transmission factor is $\psi = I_n/V_m$. Figure 2 presents the transformation from the electrical domain to optical domain with the environment described in Table 1, where $N = 2$ in ESP codes with the code weight $p = 3$ and the code size $M_s = 6$.

We first describe the matrix operation circuit in the electrical domain with $\mathbf{H} = 1/p \times \mathbf{S} \times \mathbf{BIT}$, where $\mathbf{H} = [h_0, h_1, \dots, h_{M-1}]^T$, $\mathbf{S} = [X_{1,0,0}^T, X_{1,0,1}^T, \dots, X_{N,p-1,p-1}^T, X_{N,p-1,p-2}^T]$, and $\mathbf{BIT} = [\text{bit}_0, \text{bit}_1, \dots, \text{bit}_{M_s-1}, \text{bit}_{M_s-1}]^T$. The codes are then transformed to the waveform as follows. Let h_0 denote the element of \mathbf{H} . If code $X_{1,0,0}$ is transmitted and bit_0 is 1, h_0 is 1/3. In contrast, if the codes $X_{1,0,0}$ and $X_{1,1,0}$ are transmitted and bit_0 is 1, h_0 will be 2/3. If the codes $X_{1,0,0}$, $X_{1,1,0}$, and $X_{1,2,0}$ are transmitted and bit_0 is 1, h_0 becomes 1. If the codes without $X_{1,0,0}$, $X_{1,1,0}$, and $X_{1,2,0}$ are transmitted and bit_0 is 1, h_0 is 0. Let $V_{m,max}$ denote the maximum value of modulation voltage V_m . Afterward, h_i is included in the voltage setting in the transformation to the waveform, i.e., $V_m = -V_{m,max} + 2V_{m,max}h_i$.

Figure 3 shows the receiver structure of the proposed ONU(τ) with ESP codes for TCK in an OCDMA system. The ONU(τ) comprises two sets of fiber Bragg gratings (FBGs), one balanced detector, and an integrator. The two FBG sets are constructed based on the codewords $X_{e,m,n}$ and $X_{e,m,n'}$. The upper output part is connected to the input part of the photodetector (PD) as PD0, and the lower output part is connected to the input part of PD1.¹³ The balanced detector is connected to an integrator. The two cross-correlation results $X_{e,m,n} \odot X_{f,q,r}$ and $X_{e,m,n'} \odot X_{f,q,r}$ lead to the output of PDs 0 to 1 in the balanced detector.

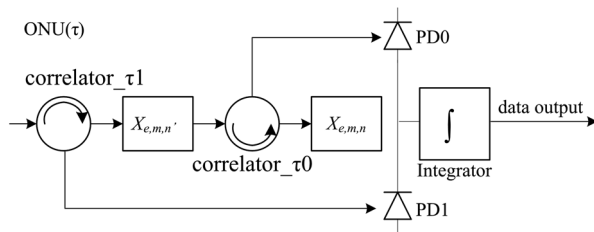


Fig. 3 The receiver structures of the ESP codes for TCK in an optical network unit (ONU, τ).

The principles of the FBG-based decoder are based on the cross-correlation described as in Eq. (1). The code sequences $X_{f,q,r}$ are first received by the FBG-based decoder. Then, the signature code $X_{e,m,n}$ achieves the modified cross correlation as shown in Fig. 3. The input of the correlator_τ1 represents the spectral components. The first output of the correlator_τ1 is connected to the FBG for the code sequence $X_{e,m,n'}$. The second output of the correlator_τ1 is connected to the PD1. The spectral components with the FBG for the code sequence $X_{e,m,n'}$ are reflected back toward the PD1 to obtain the photocurrent $I_{1,\text{bit}=x}$. The other spectral components are passed through the FBG for the code sequence $X_{e,m,n}$.

The other spectral components are connected to the correlator_τ0. The first output of the correlator_τ0 is connected to the FBG for the code sequence $X_{e,m,n}$. The second output of the correlator_τ0 is connected to the PD0. The spectral components with the FBG for the code sequence $X_{e,m,n}$ are reflected back toward the PD0 to acquire the photocurrent $I_{0,\text{bit}=x}$. The other spectral components are passed through the FBG for the code sequence $X_{e,m,n}$. The average photocurrent is $I_{r,\text{bit}=0} = I_{0,\text{bit}=0} - I_{1,\text{bit}=0}$ and $I_{r,\text{bit}=1} = I_{0,\text{bit}=1} - I_{1,\text{bit}=1}$ corresponding to Eq. (1). Therefore, the principles of the FBG-based decoder are based on the cross-correlation.

Moreover, we eliminate the MUI with Eq. (1) according to the difference between the two correlations. Now, Table 2 compares the optical power budget for the conventional OLT using SP codes and the proposed OLT.⁶ Since the proposed OLT does not include splitter and combiner, which generally have high insertion loss, the power loss of the proposed OLT is much smaller than that of the conventional ones. This replaceable word is the insertion loss of A. The insertion loss of AWG is 3 dB according to the existing work.¹⁴ By contrast, the insertion losses in this paper are improved to 5 dB for the 1×49 AWG multiplexer and 5 dB for the 49×1 AWG demultiplexer, respectively. The total insertion loss is 10 dB. This replaceable word is the insertion loss of B and insertion

Table 2 Comparison of optical power budgets for conventional OLT with SP codes and proposed OLT with ESP codes.

Items	*n	Optical PB (Ref. 6)	n	Optical PB
Code W		$p = 7$		$p = 7$
Ins. A	0	0 dB	1	10 dB
Ins. EOM	0	0 dB	1	2 dB
Ins. B	1	4 dB	0	0 dB
Ins. C	1	4 dB	0	0 dB
Ins. D	1	0.9 dB	0	0 dB
Ins. E	1	11 dB	0	0 dB
Ins. F	1	11 dB	0	0 dB
Total		30.9 dB		12 dB

Note: Optical PB: Optical Power Budget; Code W: Code Weight; Insertion loss of Ins.: A: 1×49 and 49×1 AWG (DE)MUX; B: 1×7 Coarse AWG; C: 7×7 Fine AWG; D: 2×1 Optical Switch; E: 1×7 Splitter; F: 7×1 Combiner.

loss of C. The insertion loss of AWG is 3 dB according to the literature.¹⁴ The insertion loss of 7×7 AWG is 2.4 dB according to the literature.¹⁵ By contrast, the insertion losses in this paper are improved to 4 dB for the 1×7 coarse AWG multiplexer and 4 dB for the 7×7 fine AWG, respectively. This replaceable word is the insertion loss of D. The insertion loss of the optical switch is 0.7 dB according to the existing work.¹⁶ By contrast, the insertion loss in this paper is improved to 0.9 dB for the optical switch. This replaceable word is the insertion loss of E and insertion loss of F. The insertion loss of the optical splitter (and optical combiner) is 11 dB according to the Ref. 17. Therefore, the insertion loss is 11 dB for the optical splitter (and optical combiner). This replaceable word is the insertion loss of EOM. The insertion loss of the EOM is 1.2 dB according to the existing work.¹⁸ By contrast, the insertion loss in this paper is improved to 2 dB for the EOM. The power budget difference will be increased with the value of p . Therefore, as $p = 7$, the optical power budget (dB) decreases from 30.9 dB in the SP codes in Ref. 6 to 12 dB in the proposed OLT.

3 System Performance

We first describe the signal-to-noise ratio (SNR) and bit error rate (BER) of the proposed scheme. The photocurrent noise variances are derived according to independent noise variances, i.e., $\langle i_{\text{noise,bit=0}}^2 \rangle = \langle i_{\text{PIIN,bit=0}}^2 \rangle + \langle i_{\text{shot,bit=0}}^2 \rangle + \langle i_{\text{thermal,bit=0}}^2 \rangle$ and $\langle i_{\text{noise,bit=1}}^2 \rangle = \langle i_{\text{PIIN,bit=1}}^2 \rangle + \langle i_{\text{shot,bit=1}}^2 \rangle + \langle i_{\text{thermal,bit=1}}^2 \rangle$, where the average photocurrents in the received signals are $I_{0,\text{bit=0}}$, $I_{1,\text{bit=0}}$, $I_{0,\text{bit=1}}$, and $I_{1,\text{bit=1}}$.

Note that the cross-correlation between $X_{1,0,0}$ and $X_{f,q,r}$ corresponds to the cross-correlation of the PD current $I_{0,\text{bit}=x}$ and $I_{1,\text{bit}=x}$ with information bit = “ x ”. Therefore, if the information bit is “0,” the two cross-correlations are $I_{0,\text{bit=0}}$ and $I_{1,\text{bit=0}}$. If the information bit is “1,” the two cross-correlations are $I_{0,\text{bit=1}}$ and $I_{1,\text{bit=1}}$. Before obtaining $\text{SNR}_{\text{bit=0}}$, $\text{SNR}_{\text{bit=1}}$, and BER, below we first derive the number of type-I simultaneous users, probability density function of the cross-correlation value, total cross-correlation, auto correlation, and photocurrent noise variances.

First, we derive the number of type-I simultaneous users. Let W denote the number of simultaneous users, and we randomly choose one of them as the major simultaneous user, which selects $X_{1,0,0}$ code, whereas other $(W - 1)$ simultaneous users will select other codes. The number of type-I simultaneous users is $\lceil (W - 1)/N \rceil$ because $\lceil (W - 1) - (W - 1)/N \rceil$ simultaneous users have the cross correlation as “0.”

Second, we derive the probability density function of the cross-correlation value with “1” and “0.” The code weight is p , and p is odd. $(p - 1)$ is the even because we adopt $(p - 1)$ divided by 2 from the TCK, and the remainder is zero. The code size is $M_s = N(p^2 - p)/2$ in TCK. The probability density function of the cross-correlation value with “0” is $[(p - 1)/2 - 1]/[(p^2 - p)/2 - 1]$. The probability density function of the cross-correlation value with “1” is $[1 - [(p - 1)/2 - 1]/[(p^2 - p)/2 - 1]]$.

Third, we derive the total cross-correlation. Before the derivation of the PD current, the total cross-correlation is $\Lambda = \lceil (W - 1)/N \rceil - \lfloor \lceil (W - 1)/N \rceil (p - 3)/(p^2 - p - 2) \rfloor$, where the cross-correlation value is “0” and “1,” the number

of type-I simultaneous users is $\lceil (W - 1)/N \rceil$, and the probability density function of the cross-correlation value is set with “0” and “1.”

Fourth, we derive the auto-cross correlation. $(p + \Lambda)$ is the auto-cross correlation adding to the total cross-correlation. The code length (Np^2) is incorporated in $(p + \Lambda)/(Np^2)$. The average photocurrents $I_{0,\text{bit=0}}$, $I_{1,\text{bit=0}}$, $I_{0,\text{bit=1}}$, and $I_{1,\text{bit=1}}$ are originated as follows. For information bit = “0” we develop $I_{0,\text{bit=0}}$ and $I_{1,\text{bit=0}}$ as $I_{0,\text{bit=0}} = \text{RP}_{\text{sr}}(p + \Lambda)/(Np^2)$ and $I_{1,\text{bit=0}} = \text{RP}_{\text{sr}}\Lambda/(Np^2)$. For information bit = “1” we develop $I_{0,\text{bit=1}}$ and $I_{1,\text{bit=1}}$ as $I_{0,\text{bit=1}} = \text{RP}_{\text{sr}}\Lambda/(Np^2)$ and $I_{1,\text{bit=1}} = \text{RP}_{\text{sr}}(p + \Lambda)/(Np^2)$. As the information bit = “0” and “1,” the average photocurrent is as follows:

$$\begin{aligned} I_{r,\text{bit=0}} &= I_{0,\text{bit=0}} - I_{1,\text{bit=0}} = \text{RP}_{\text{sr}}/(Np) \quad \text{and} \\ I_{r,\text{bit=1}} &= I_{0,\text{bit=1}} - I_{1,\text{bit=1}} = -\text{RP}_{\text{sr}}/(Np), \end{aligned} \quad (2)$$

where R is the responsivity of the photodiode.

Fifth, we derive the variance of the PIIN, shot noise, and thermal noise. According to the statistically independent noise characteristics, the variance of the PIIN current at each ONU receiver is as follows:

$$\begin{aligned} &< i_{\text{PIIN,bit=0}}^2 \rangle \\ &= B_r R^2 P_{\text{sr}}^2 p [(1 + \Lambda/p)^2 + (\Lambda/p)^2] / (\Delta f N p^2) \\ &= B_r R^2 P_{\text{sr}}^2 \{1 + 2\Lambda/p + 2\Lambda^2/p^2\} / (\Delta f N p), \end{aligned} \quad (3)$$

where $\langle i_{\text{PIIN,bit=1}}^2 \rangle = \langle i_{\text{PIIN,bit=0}}^2 \rangle$. The above equations show that the ESP codes can increase the number of simultaneous users because the variance of PIIN current is reduced by N . Thus, the power of PIIN is also suppressed. Since shot noise is obtained from the mutually independent PDs 0 and 1, the variance in the shot noise current is expressed as

$$\begin{aligned} &< i_{\text{shot,bit=1}}^2 \rangle = 2eB_r(I_{0,\text{bit=0}} + I_{1,\text{bit=0}}) \quad \text{and} \\ &< i_{\text{shot,bit=1}}^2 \rangle = 2eB_r(I_{0,\text{bit=1}} + I_{1,\text{bit=1}}). \end{aligned} \quad (4)$$

Moreover, the variance of the thermal noise current is as

$$\langle i_{\text{thermal,bit=0}}^2 \rangle = \langle i_{\text{thermal,bit=1}}^2 \rangle = 4K_b T_n B_r / R_L. \quad (5)$$

Finally, we derive the $\text{SNR}_{\text{bit=0}}$, $\text{SNR}_{\text{bit=1}}$, and BER. We utilize the Gaussian approximation to find the BER, while the SNRs are $\text{SNR}_{\text{bit=0}} = I_{r,\text{bit=0}}^2 / \langle i_{\text{noise,bit=0}}^2 \rangle$ and $\text{SNR}_{\text{bit=1}} = I_{r,\text{bit=1}}^2 / \langle i_{\text{noise,bit=1}}^2 \rangle$. Therefore, the BER is obtained as $\text{BER} = \text{erfc}(\sqrt{(\text{SNR}_{\text{bit=0}} \text{ or } \text{SNR}_{\text{bit=1}})/2})/2^6$.

Figure 4 shows the numerical results with $\Delta f = 12.5$ TGz, $\lambda_0 = 1.55$ μm , the data transmission rate = 2.5 Gbps, $T_n = 300$ K, and $R_L = 1030$ Ω . The B_r of the receiver is half of the data transmission rate. Figure 4 compares the proposed ESP codes and SP codes with similar code lengths. We use the effective source power and data transmission rate to present -5 dBm and 2.5 Gbps, respectively. The code weight is set as $p = 5$, $N = 14$, $p = 5$, and $N = 8$ in the ESP codes for TCK. The results indicate that the maximum number of simultaneous users for $p = 5$ and $N = 14$ in our proposed system can reach 60 as $\text{BER} = 10^{-9}$.

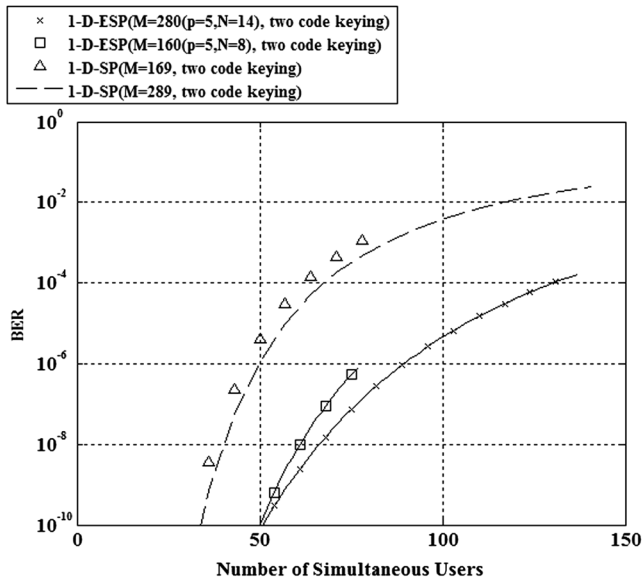


Fig. 4 Comparison of bit error rate (BER) in the proposed ESP and other codes with different numbers of simultaneous users.

4 Conclusion

We propose ESP codes and demonstrate that the effects of PIIN are effectively suppressed. Compared with the existing SP codes, our numerical results show that ESP codes can effectively increase the number of simultaneous users under 2.5-Gbps data transmission. Moreover, a universal OLT encoding architecture can be operated with other code families. Then, we also devise a AWG architecture for ESP codes to reduce the power loss and the complexity for OLT in PONs.

Acknowledgments

The authors wish to thank the High Speed Intelligent Communication (HSIC) Research Center at the Chang Gung University, Taiwan, for providing facilities and financial support which were crucial to our study.

References

1. Z. Wang et al., "Optical encryption with OCDMA code swapping using all-optical XOR logic gate," *IEEE Photonics Technol. Lett.* **21**(7), 411–413 (2009).
2. H. Chen et al., "A tunable encoder/decoder based on polarization modulation for the SAC-OCDMA PON," *IEEE Photonics Technol. Lett.* **23**(11), 748–750 (2011).

3. V. Jyoti and R. S. Kaler, "Isolated user security enhancement in optical code division multiple access network against eavesdropping," *Opt. Eng.* **51**(9), 09501 (2012).
4. B. M. Ghaffari, M. D. Matinfar, and J. A. Salehi, "Wireless optical CDMA LAN: digital implementation analysis," *IEEE J. Sel. Areas Commun.* **27**(9), 1676–1686 (2009).
5. M. Xin et al., "Multipolar inserting zeros code and its application in optical code division multiple access systems," *Opt. Eng.* **46**(2), 020501 (2007).
6. C. C. Yang, "Optical CDMA passive optical network using prime code with interference elimination," *IEEE Photonics Technol. Lett.* **19**(7), 516–518 (2007).
7. C.-C. Yang, "Spectral efficiencies of the optical CDMA-based PONs using two-code keying," *IEEE Commun. Lett.* **14**(8), 767–769 (2010).
8. C.-C. Yang, "Code space enlargement for hybrid fiber radio and base-band OCDMA PON," *Lightw. Technol.* **29**(9), 1394–1400 (2011).
9. C.-C. Yang, "Hybrid wavelength-division-multiplexing spectral-amplitude-coding optical CDMA system," *Photonics Technol. Lett.* **17**(6), 1343–1345 (2005).
10. S.-M. Lin, J.-F. Huang, and C.-C. Yang, "Optical CDMA network codecs with merged-M-coded wavelength-hopping and prime-coded time-spreading," *Opt. Fiber Technol.* **13**(2), 117–128 (2007).
11. C.-C. Yang, J.-F. Huang, and S.-P. Tseng, "Optical CDMA network codecs structured with M-sequence codes over waveguide-grating routers," *Photonics Technol. Lett.* **16**(2), 1041–1135 (2004).
12. M. Bass, *Handbook of Optics*, 3rd ed., Vol. 3, McGraw-Hill Professional (2010).
13. J. W. Goodman, *Statistical Optics*, Wiley, New York, California (1985).
14. W. Bogaerts et al., "Silicon-on-Insulator Spectral Filters Fabricated With CMOS Technology," *IEEE J. Sel. Top. Quant. Electron.* **16**(1), 33–44 (2010).
15. K. A. McGreer, "Arrayed waveguide gratings for wavelength routing," *IEEE Commun. Mag.* **36**(12), 62–68 (1998).
16. R. T. Chen, H. Nguyen, and M. C. Wu, "A high-speed low-voltage stress induced micromachined 2x2 optical switch," *IEEE Photonics Technol. Lett.* **11**(11), 1396–1398 (1999).
17. Y. Hibino et al., "High reliability optical splitters composed of silica-based planar lightwave circuits," *Lightw. Technol.* **13**(8), 1728–1735 (1995).
18. T. H. Wood et al., "131 ps optical modulation in semiconductor multiple quantum wells (MQW's)," *IEEE J. Quantum Electron.* **21**(2), 117–118 (1985).

Bih-Chyun Yeh received his BS, MS, and PhD degrees in communication engineering from National Taiwan University, Taipei, Taiwan, in 1996, 1998, and 2009, respectively. He is now an assistant professor in the Faculty of Chang Gung University. His research interests include the lightwave and wireless communication systems.

Cheing-Hong Lin received his BS degree in communication engineering from National Chiao Tung University, in 1997, and his MS and PhD degrees in communication engineering from National Taiwan University, Taipei, Taiwan, in 1999 and 2005, respectively. His current research interests include lightwave and wireless communication systems and computer networks.

De-Nian Yang received his BS and PhD degrees from the Department of Electrical Engineering, National Taiwan University, Taipei, Taiwan, in 1999 and 2004, respectively. He is now an associate research fellow in the Institute of Information Science, Academia Sinica. His research interests include multimedia and mobile networking, social networks, theoretical rigor, and practical feasibility.